SUPPLEMENTARY INFORMATION

Combating the amyloid-induced cellular toxicity and stiffness by designer peptidomimetics

Mouli Konar,[‡a] Debasis Ghosh,[‡a] Sourav Samanta[a] and Thimmaiah Govindaraju*[a]

Bioorganic Chemistry Laboratory, New Chemistry Unit and School of Advanced Materials (SAMat),

Jawaharlal Nehru Centre for Advanced Scientific Research, Jakkur P.O., Bengaluru 560064, Karnataka, India.

Corresponding Author (T.G.): tgraju@jncasr.ac.in

Table of Contents

Experimental section

General methods

All solvents and reagents were obtained from Spectrochem or Merck and used without further purification unless mentioned. Dulbecco's Modified Eagle Medium/Nutrient Mixture F12 (DMEM F12), Roswell Park Memorial Institute (RPMI), fetal bovine serum (FBS) and Alamar blue was obtained from Invitrogen. Amyloid beta (Aβ42) peptide (PP69-0.05 MG), anti-amyloid fibrils (OC) and fluorescently labelled secondary antibody were obtained from Merck. Thioflavin T (ThT) was obtained from Sigma-Aldrich (T3516) and DAPI (4′,6-diamidino-2-phenylindole) from Vector Laboratories, CA, USA (H-1200). Agilent Cary eclipse fluorescence spectrophotometer and microplate reader (SpectrsMax i3x) were used for fluorescence assays. A Bruker IFS 66/V spectrometer and JASCO-815 spectropolarimeter were employed to perform Fourier Transform Infrared (FTIR) and circular dichroism (CD) spectroscopy studies, respectively. ^{1}H and ^{13}C NMR spectra were recorded in Bruker AV−400 and JEOL-600 MHz spectrometers using tetramethylsilane (TMS) as internal standard. MALDI-TOF, HRMS, LCMS and HPLC spectra were acquired from Bruker Autoflex Speed MALDI-TOF spectrometer, Agilent 6538 UHD HRMS/Q-TOF high-resolution spectrometer, Shimadzu LCMS-2020 and SHIMADZU reverse phase HPLC (using C18 column), respectively. A mixture of acetonitrile and water was used as mobile phase in HPLC and the peptide or peptidomimetics were collected using PDA detector (absorbance at 254 nm). Confocal images were captured using confocal fluorescence microscope (Olympus FV3000). Calculated amount of Aβ14-23 (I), Akd^{M} (II), Akd^{C} (III), Akd^{N} (IV), and Akd^{NMC} (V) were dissolved in hexafluoroisopropanol (HFIP, 200 μL), followed by the removal of HFIP under nitrogen atmosphere, and dried under vacuum to obtain monomeric peptide/peptidomimetics samples. Glycine-HCl buffer (10 mM) and phosphate buffer saline (10 mM) prepared in water (passed through 0.22-micron

filter, conductivity at 25 °C < 100 µS/cm, Milli Q) were used for maintaining the solution pH at 2.0 and 7.4, respectively. The experimental raw data were processed using Origin 8.5, Prism 6 or ChemDraw professional 15.

Synthesis of Aβ14-23 (I) peptide and CDP-peptidomimetics (II-V)

The cyclic dipeptide (CDP) [cyclo(Lys-Asp)]-based unnatural amino acid (kd) was synthesized by 9-fluorenylmethoxycarbonyl (Fmoc)-deprotection of dipeptide Fmoc-Lys(Boc)-Asp(O*t*Bu)-OMe followed by the cyclization and deprotection of Boc-protecting groups. Aβ14-23 (I) and kd-incorporated Aβ14-23 peptidomimetics Akd^{M} (II), Akd^{C} (III), Akd^{N} (IV), Akd^{NMC} (V) were synthesized following standard Fmoc solid phase peptide synthesis (SPPS) protocol. Fmoc-amino acids (H: Histidine, Q: Glutamine, K: Lysine, L: Leucine, V: Valine, F: Phenyl alanine, A: Alanine, E: Glutamic acid, and D: Aspartic acid) with *t*Boc and *t*But protection on the side chains of the respective -NH_2 and -COOH functionalities were used to synthesize the peptide or peptidomimetics. Rink amide resin (loading 0.76 mmol/gm) was employed as the solid support in SPPS. For the coupling of Fmoc-amino acids (2.5 eq.) and Fmoc-kd (2.5 eq.) in the desired peptide sequence, HBTU (2.5 eq.)-HOBt (2.5 eq.), DIPEA (4 eq.) and DMF were used as activating agent, base, and solvent, respectively. The completion of the coupling and Fmoc-deprotection of amino acids were confirmed by Kaiser test. After every coupling and deprotection step, resin was thoroughly washed with DMF and DCM. The synthesized peptide or peptidomimetics were cleaved from the resin using a cleavage-cocktail solution of TFA: TIPS: DCM (95:2.5:2.5) at room temperature and the product was collected through precipitation from cold diethyl ether. All the synthesized peptide or peptidomimetics were finally purified by reverse phase HPLC (C18 column) using acetonitrile: water system and the product purity and integrity were ascertained by analytical HPLC and HRMS. ^{1}H NMR (400 MHz, DMSO-d_6) δ (ppm): 1.30 (4H, m); 1.68 (2H, m); 2.61-2.63 (2H, m); 2.95-2.97 (2H, d, J = 8 Hz);

3.88 (1H, s); 4.18-4.20 (2H, d, J = 8 Hz); 4.22 (2H, s); 7.23-7.43 (9H, m); 8.0 (1H, s); 8.19 (1H, s). ^{13}C NMR (100 MHz, DMSO-d_6): δ (ppm): 21.4, 29.2, 31.3, 36.5, 38.8, 40.1, 46.7, 50.9, 53.8, 65.2, 120.1, 125.1, 127.0, 127.5, 140.7, 143.9, 156.9, 167.5, 168.1, 171.3. HRMS (ESI-TOF) m/z: $[M + H]^+$ calculated for $C_{25}H_{28}N_3O_6$, 466.1978; observed 466.1970.

Circular Dichroism (CD) studies

The changes in secondary structural conformations of peptide I upon aggregation in the absence and presence of peptidomimetics (II-V) were monitored by CD spectroscopy. To record the CD spectra, peptide I (25 μM) was incubated in the presence and absence of peptidomimetics (25 μM) at 37 °C for 20 days at pH 2.0 (10 mM) and 7.4 (10 mM). A quartz cuvette of path length 0.1 cm was used, and the spectra were recorded in the wavelength range of 190 - 240 nm at 50 nm/min scan rate. For CD analyses, the background correction was performed using the CD spectrum recorded in only PBS buffer.

Fourier-Transform Infrared Spectroscopy (FTIR) studies

For FTIR spectroscopy studies, aliquots (10 μL) of peptide I (25 μM) incubated with and without peptidomimetics (25 μM) at 37 °C for 20 days at pH 2.0 (10 mM) and 7.4 (10 mM) were independently placed on clean dry coverslips to form thin film. The FTIR spectra of the dried thin film samples were recorded at room temperature in the spectral range of 4000 - 400 cm^{-1} using FT-IR Spectrometer (Model: Bruker IFS 66/V spectrometer, Mode: ATR). A Dimond ATR was used for the acquisition of 100 spectra. A spectrum against air was used for the background correction of FTIR spectra.

Transmission electron microscopy (TEM) imaging

For TEM imaging, the pre-incubated Aβ14-23 samples (25 μM) in the absence and presence of II-V (25 μM) were diluted to 5 μM and placed on a carbon-coated copper

grid of 200 mesh size and negatively stained with 0.2 % uranyl acetate. Prior to imaging, the sample-containing grids were washed twice with purified water (MiliQ) and dried in a desiccator under nitrogen atmosphere. Finally, the imaging was performed in JEOL JEM 3010 TEM.

Docking studies

Molecular docking studies were performed using AutoDock Vina software (Version: 1.1.2).[1] The crystal structure of Aβ42 peptide (PDB ID: 1Z0Q, protein) was retrieved from RCSB Protein Data Bank and a full chain of Aβpeptide (1-42) was selected for the docking. The PDB structure of Aβ14-23 (I, protein) was created from Aβ42 using AutoDock tools. The PDB structure of Akd^{NMC} (V, ligand) was created and optimized through energy minimization in Avogadro software applying the MMFF94 force field. Gasteiger partial charges and polar hydrogen were added using AutoDock tools. For the I:V and Aβ42:V docking experiments, the entire protein domains (I and Aβ42) were covered with the grid box of dimensions 48Å X 46Å X 34 Å and 126Å X 62Å X 58Å, respectively. The total number of run involved in the docking experiment was determined by the exhaustiveness parameter which was set to a maximum value of 8 on the scale of 1–8, while keeping all other parameters as default.[2] After the completion of docking runs (I:V and Aβ42:V), the energy minimized docked poses were viewed and analysed using *PyMOL* software.

AFM imaging of Aβ-aggregates using PF QNM-AFM

The PF QNM-AFM study was performed to visualize the aggregation species of Aβ14-23 (I) or Aβ42 in the absence and presence of peptidomimetics. For the experiment, we have diluted the pre-incubated stock solutions of peptides (25 μM, I, I+II, I+III, I+IV, I+V, Aβ42, Aβ42+V) to a concentration of 5 μM and placed on freshly cleaved mica foils to dry them at room temperature. The AFM images were acquired in Bruker BIOSCOPE Resolve with PeakForce Tapping AFM instrument. A silicon nitride tip

(SCANASYST-ATR, force constant: 21-98 Nm^{-1}) of length 115 μm and resonance frequency 146-236 kHz was used. The AFM images were processed and analysed using NanoScope 1.8 analysis software (Bruker, Inc.).

Cytotoxicity assay

The cytotoxicity of peptidomimetics was determined using Alamar blue assay in *SH-SY5Y* cell line (Source: the American Type Culture Collection). At first, the cells were cultured in 96-well plate (15,000 cells/well) using DMEM/F-12 medium (Gibco, Invitrogen) containing FBS (10%) and PS (1%). Then the cell media was replaced with low serum (2% FBS) containing DMEM/F-12 media. Next, the cells were exposed to the peptidomimetics (10 μM), which were preincubated (24 h, 37 °C) at pH 7.4 for 24 h in the cell growing conditions. Finally, experimental cells were treated with Alamar blue solution for 2 h at 37 ºC and the absorbance was measured at 570 nm using microplate reader. The data were plotted and analysed using GraphPad prism software (One way ANOVA).

Live-dead assay

The well plates were seeded with the *SH-SY5Y* cells. The seeded cells were independently treated with Aβ42 (10 μM) and Aβ42+V (1:1) solutions. Cells treated with 0.1% Triton-X and untreated cells were considered as positive and negative controls, respectively. After a single wash with 1X PBS, the untreated and treated cells were stained with of calcein-AM (2μM) and propidium iodide (4.5 μM) in a 5 percent CO_2 environment for 15 min at 37 °C. The excess dyes were removed by washing the cells in 1X PBS, and images were acquired using a Leica DM2500 fluorescence microscope using 20X objective. A band-pass filter for calcein-AM (at 500-550 nm) and a long-pass filter for propidium iodide (at 590-800 nm) were used for imaging.

Intracellular ROS measurement

The *SH-SY5Y* cells were seeded at a density of 12,000 cells/well in a 96-well plate in DMEM/F-12 medium (Gibco, Invitrogen) with foetal bovine serum (FBS; 10%), horse serum (HS; 5%), and pen-strep (1 percent; Genetix) at 37 °C in a CO_2 atmosphere of 5% to assess the effects of peptidomimetics (V) on ROS generated by Aβ42-Cu^{II} using 2,7- dichlorodihydrofluorescein diacetate (DCFDA; Invitrogen). The cells were grown for 18 h, the media was changed to low serum DMEM, followed by further incubation of 6 h. The cells were then rinsed in PBS and treated with DCFDA dissolved in DMEM medium for 30 min. The cells were washed and treated with Aβ42 peptide (10 μM), Cu^{2+} (10 μM), and ascorbate (300 μM) in absence and presence of 10 μM of peptidomimetics V for 6 h at 37°C. For metal independent assay, cells were independently treated with exogenous H_2O_2 (100 μM) and H_2O_2+V (1:1). The cells were rinsed in PBS, and the DCF fluorescence intensity was assessed using excitation and emission wavelengths of 495 and 529 nm, respectively (significance was determined using GraphPad prism's one-way ANOVA).

Enzymatic stability assay

The enzymatic stability of Aβ14-23 and Akd^{NMC} was preformed against trypsin. Aβ14-23 (100 μM) and Akd^{NMC} (100 μM) were independently incubated with 5 μM trypsin in tris-HCl (10 mM, pH 8) buffer at 37 °C under shaking conditions. After 24 h, the reaction was halted with 0.05% formic acid. The amount of intact peptide/peptidomimetics was analysed using analytical HPLC (SHIMADZU LCMS-2020).

Results and discussion

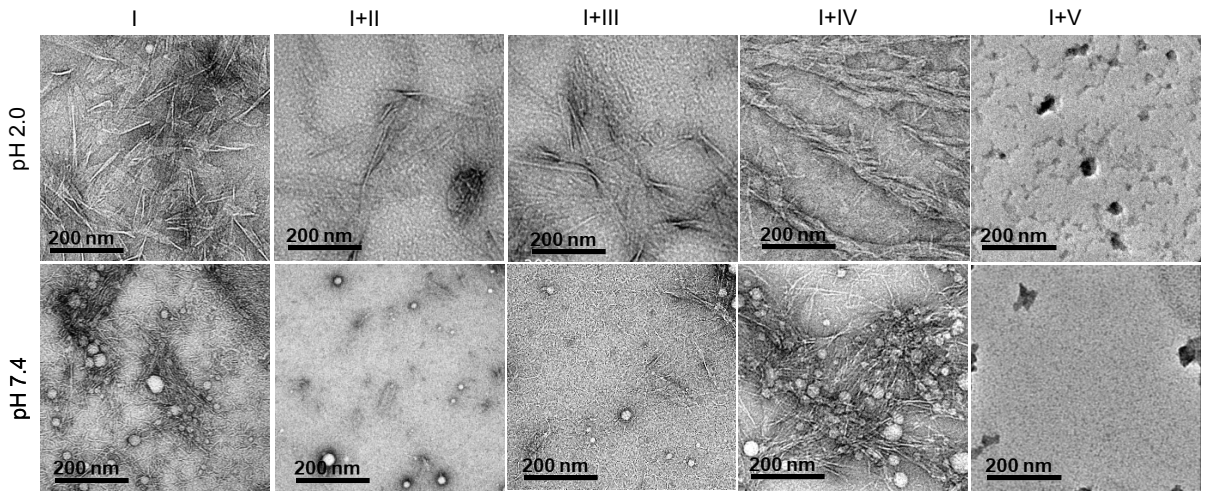

Fig. S1 TEM images of pre-incubated I in the absence and presence of II-V at pH 2.0 and 7.4.

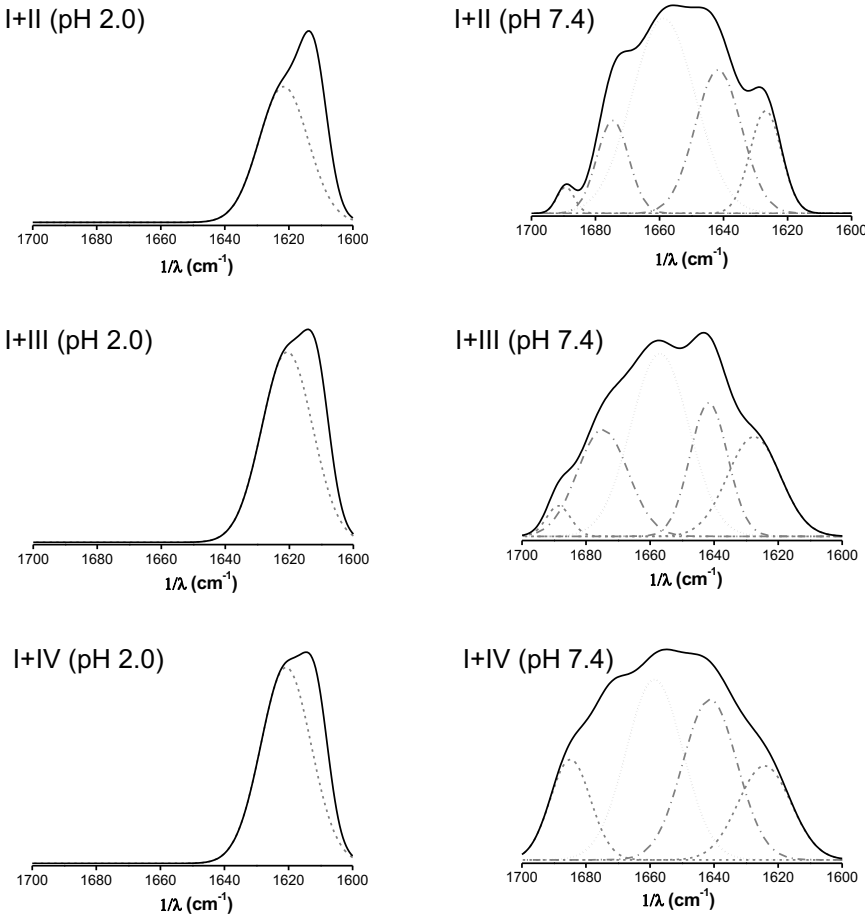

Fig. S2 FTIR spectra of pre-incubated I (25 μM) in the absence and presence of peptidomimetics II-IV (25 μM) at pH 2.0 and 7.4. (dottedline: α-helix, dotted-dashed line: Random coil; dashed line: β-Sheet)

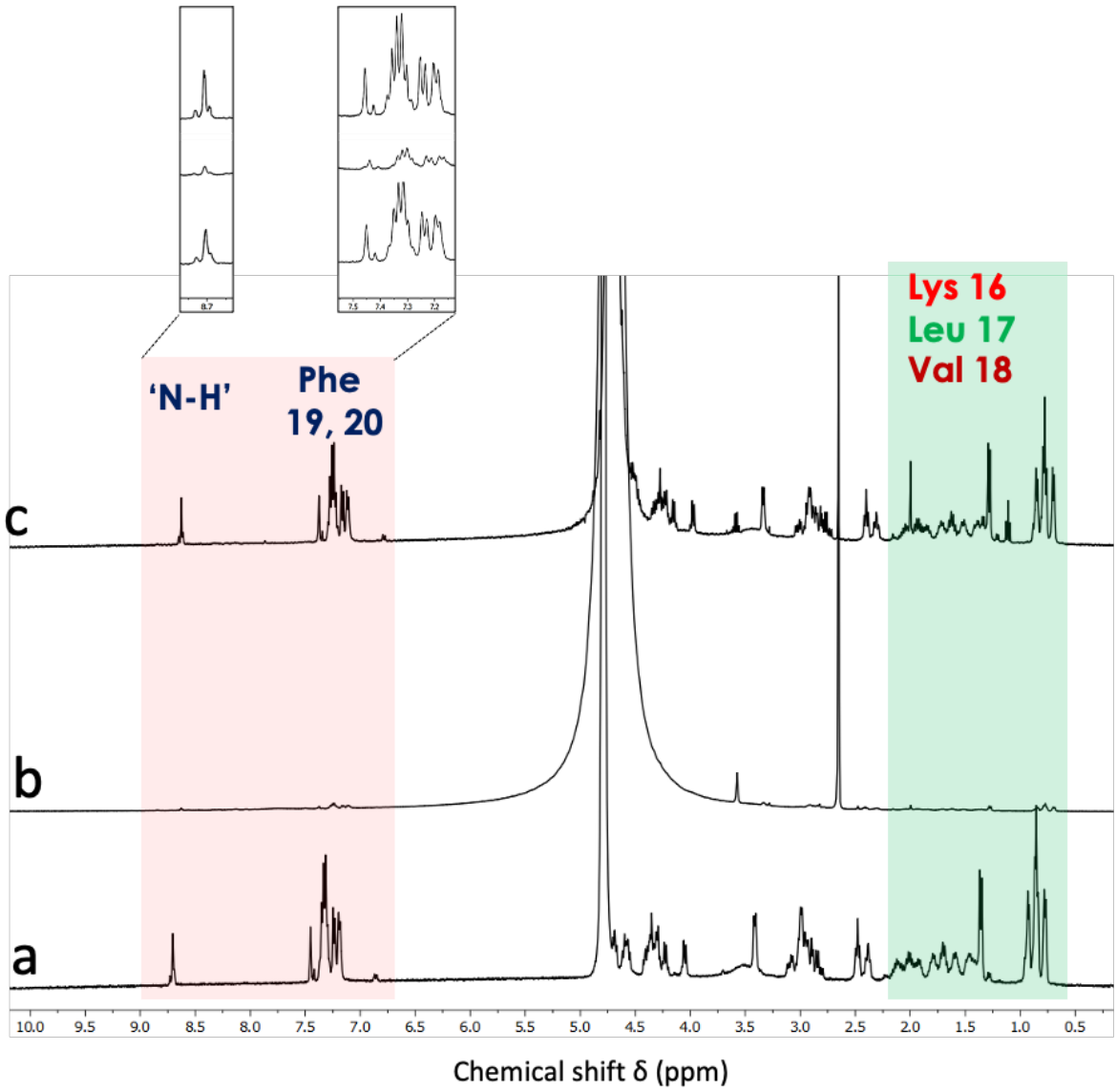

Fig. S3 (a) ^{1}H NMR spectrum of Aβ14-23 (I) at room temperature show a broad range of chemical shifts confirming its native monomer conformation. (b) The spectral features of fibrillar Aβ14-23 show the disappearance of most of the amide and aromatic (Phe 19, 20) proton signals, which suggest the fibril formation. (c) ^{1}H NMR spectrum of solution containing an equimolar ratio of Akd^{NMC} (V) and I, which show well-distributed protons with a broad range of chemical shifts comparable to that of control sample (monomer) of I (a). The observed proton signals of I similar to monomer conformation in the presence of V confirmed the stabilization of monomeric state of Aβ14-23 (I) by V.

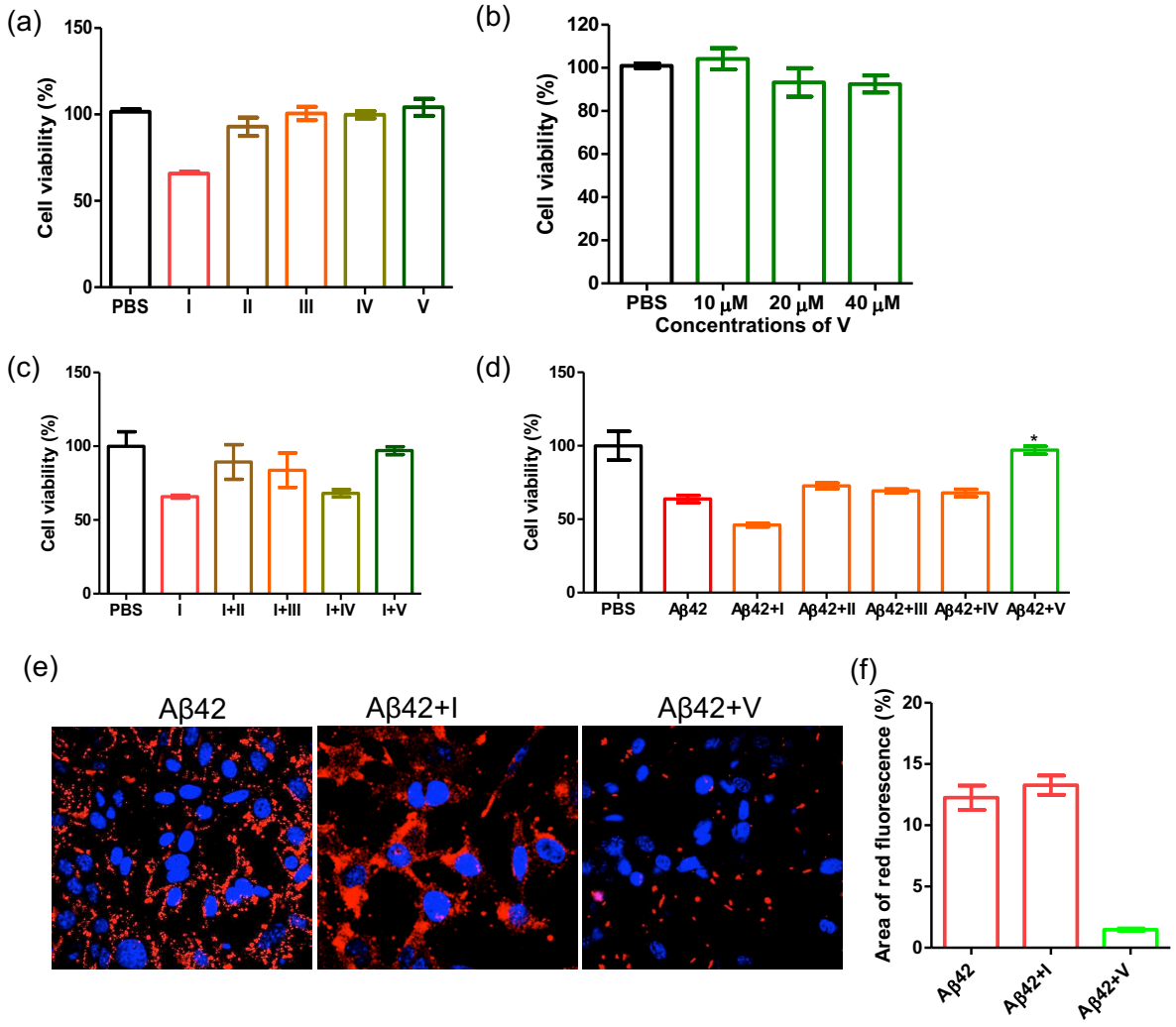

Fig. S4 Cytotoxicity of peptidomimetics and their neuronal rescue ability from amyloid-induced cellular stress. (a) The cell viability of the *SH-SY5Y* after treating (24 h) with PBS buffer (10 mM), I (10 μM) and peptidomimetics II-V (10 μM) at pH 7.4. The result confirmed that peptidomimetics are nontoxic to neuronal cells, while Aβ14-23 (I) exhibited significant amyloidogenic toxicity. (b) The cell viability of the *SH-SY5Y* after treating (24 h) with PBS buffer (10 mM) and different concentrations of V (10-40 μM), which indicate relatively non-toxic nature of V in that concentration range. (c) The cell viability of *SH-SY5Y* after treating (24 h) with PBS, pre-incubated (48 h) I (10 μM) alone and with peptidomimetics (II-V) at pH 7.4. The result confirmed the potential of peptidomimetic II and V to rescue the neuronal cells. (d) The cell viability of the *SH-SY5Y* after treating (24 h) with PBS, pre-incubated (48 h) Aβ42 (10 μM) in the absence and presence of peptidomimetic I-V (10 μM) at pH 7.4. The result confirmed that peptidomimetic V is the most potent to rescue the neuronal cells from amyloid-induced cytotoxicity. (e) Confocal images of immunostained *SH-SY5Y* cells with OC and secondary antibody (red). Blue: nuclear staining with DAPI in the presence of Aβ42, Aβ42+I, Aβ42+V samples. Scale bar: 20 μm. (F) Representative bar plot indicating total cytotoxic area (% area of red fluorescence) for the samples Aβ42, Aβ42+I, and Aβ42+V in (e), which proved that I induced membrane-localized amyloid aggregates formation and V act as a potent inhibitor of amyloid aggregation.

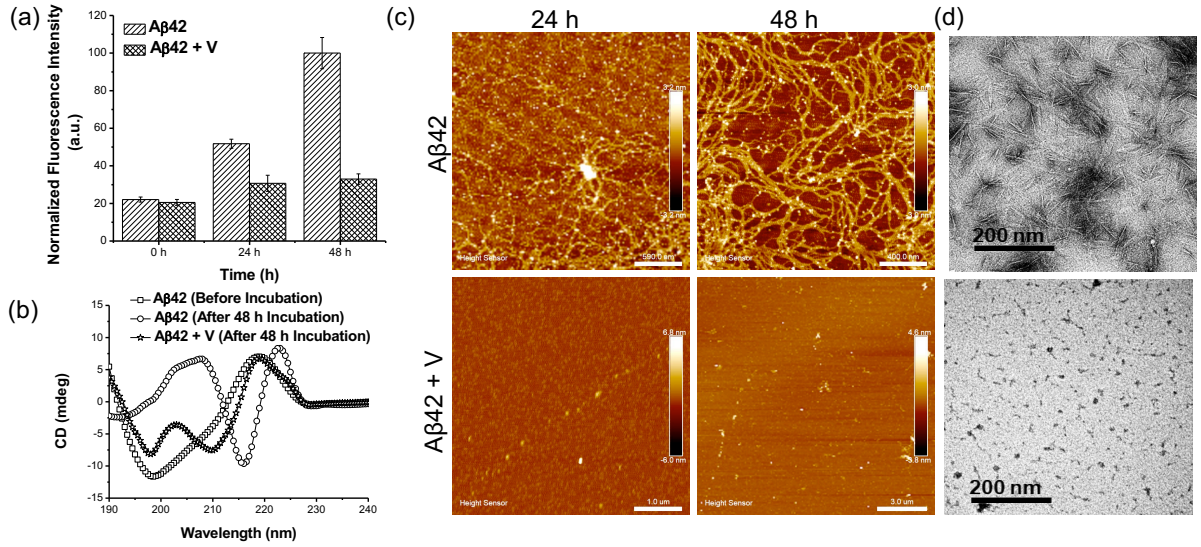

Fig. S5 Aβ42 aggregation in the presence and absence of Akd^{NMC} (V) in phosphate buffer saline (PBS) conditions (pH 7.4) at 37 °C over a period of 2 days. (a) Time-dependent ThT fluorescence assay data (λ_{em} = 482 nm) showed inhibition of Aβ42 aggregation in the presence of V. (b) CD spectra of Aβ42 in the absence and presence of V show Aβ42 aggregation with β-sheet conformation in the absence of V after 48 h incubation, while inhibitor V induced stabilization of Aβ42 through α-helical (content) conformation. (c,d) AFM and TEM images of pre-incubated Aβ42 and Aβ42+V in PBS (pH 7.4) that confirmed the inhibition of Aβ aggregation by V.

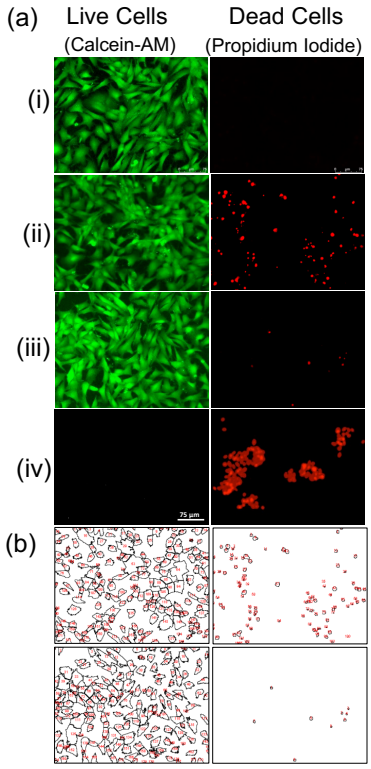

Fig. S6 (a) Fluorescence microscopy images of *SH-SY5Y* cells in Live/Dead staning assay upon treatment with Aβ42 and Aβ42+V for 24 h, Panel (i): untreated cells (negative control); panel (ii) cells treated with Aβ42 (10 μM); panel (iii): cells treated with Aβ42+V (1:1); panel (iv): cells treated with 0.1% Triton X (positive control); Scale bar is 75 μm. (b) The amount of dead cells for Aβ42, Aβ42+V-treated samples are 36% and 4 %, respectively. Images are quantified using ImageJ software.

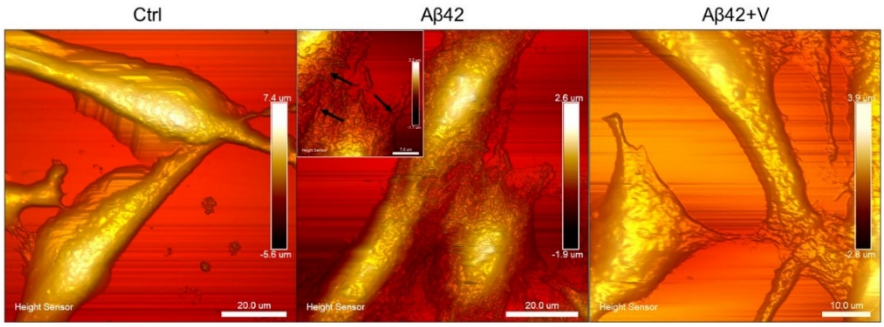

Fig. S7 PF QNM-AFM images of SH-SY5Y cells (colony) treated with PBS (Ctrl, 10 mM), Aβ42 (10 μM), Aβ42+V (10 μM, 1:1) for 24 h at pH 7.4. These AFM images confirmed the amyloid stressinduced membrane damage in neuronal cells, which can be reduced in the presence of peptidomimetic V (Akd^{NMC}). Inset in Aβ-treated cells clearly show stress fiber formation due to the emergence of amyloid-induced cellular stress uponAβ-membrabe interactions. The treatment of the peptidomimetics V on the Aβ-treated cells rescues the neuronal cells from the amyloid-induced cellular stress.

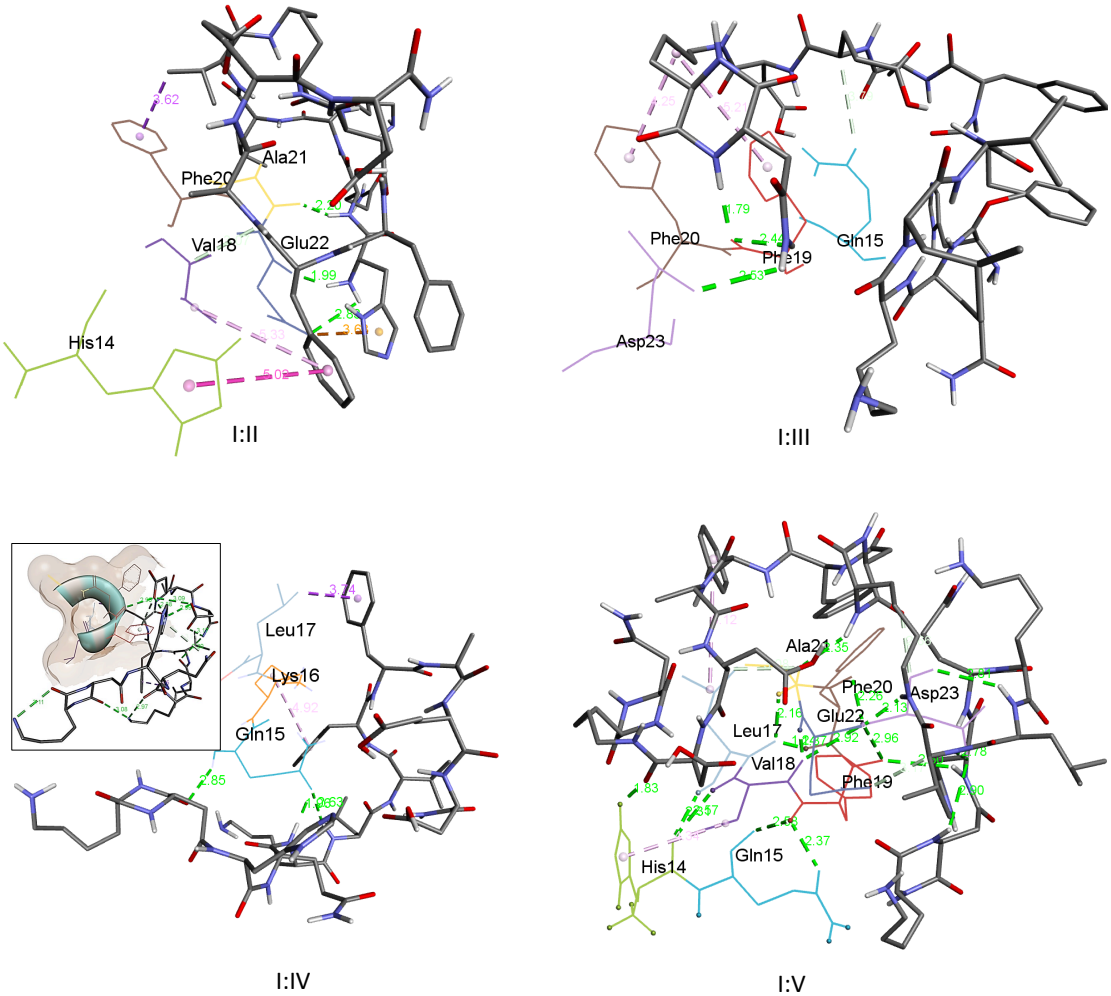

Fig S8 Representative docked structures with the residue-specific intermolecular interactions for I:II, I:III, I:IV (inset shows intensive intramolecular interactions within IV that makes it too inflexible to stabilize the hydrophobic region (surface presentation) of I leading to induced aggregation), and I:V (I : line representation), II-V : stick representation, grid dimension: 48Åx46Åx34Å). The docking results indicate that II, III, IV, and V bind to I with binding energies of -4.1, -4.1, -3.1, and -4.9 kcal/mol, respectively. Considering the binding energies and the number of hydrogen bonding interactions, V was found to be the best interacting and stabilizing inhibitor of I. Detailed binding interaction are shown in Table S4

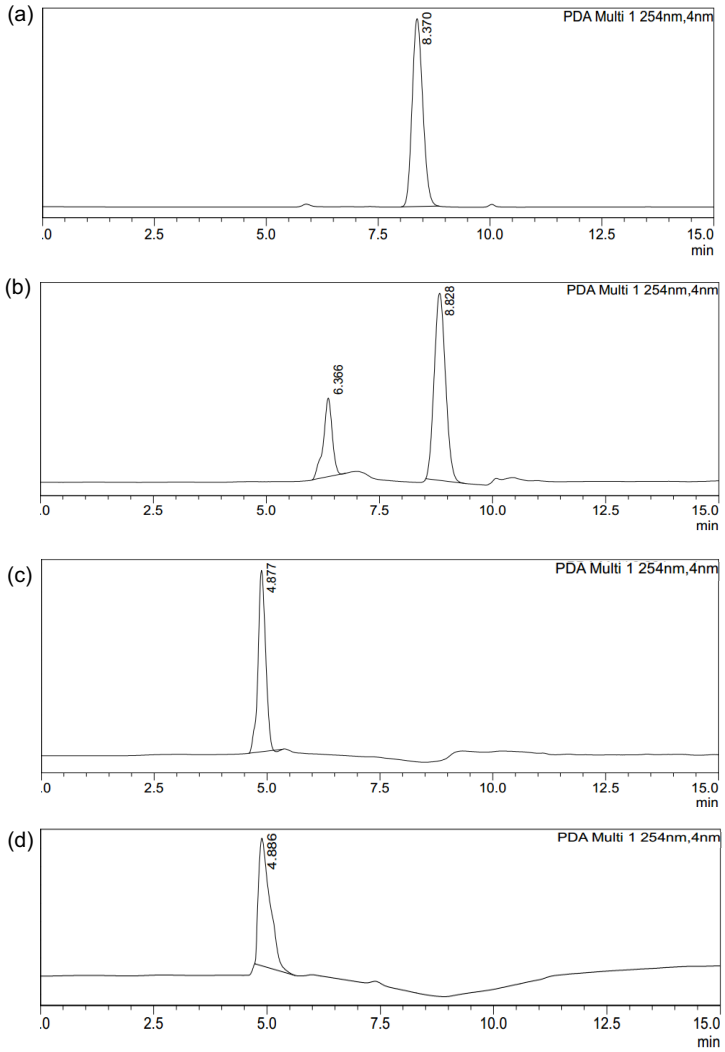

Fig. S9 Stability of Aβ14-23 (100 μM) and Akd^{NMC} (100 μM) against the enzymatic degradation (trypsin, 5 μM). (a) and (b) Analytical HPLC data of Aβ14-23 before and after the incubation (24 h) with trypsin, respectively. (c) and (d) Analytical HPLC data of Akd^{NMC} before and after the incubation (24 h) with trypsin, respectively. The chromatogram confirms that Akd^{NMC} is stable against enzymatic degradation, which satisfies the design strategy.

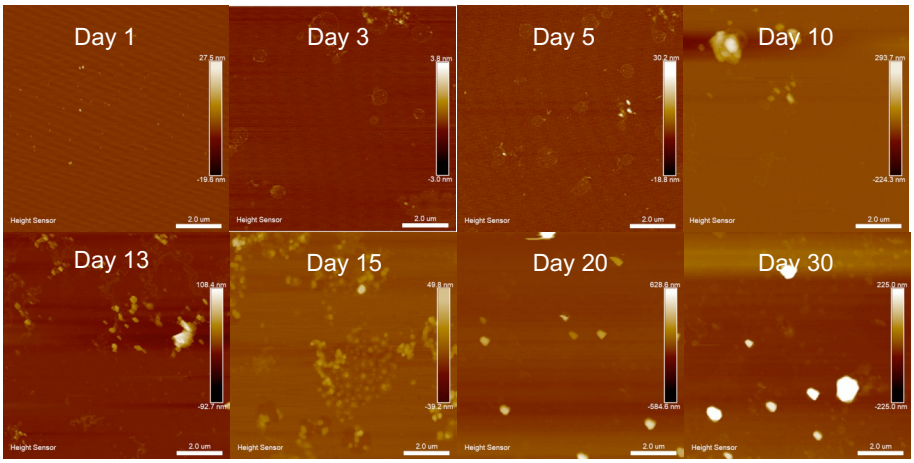

Fig. S10 Time-dependent AFM images of V (5 μM) incubated independently in PBS (10 mM) at pH 7.4 and 37 °C for 30 days. The prolonged time incubation of the peptidomimetics V with no aggregation species confirms its non-self-aggregating nature.

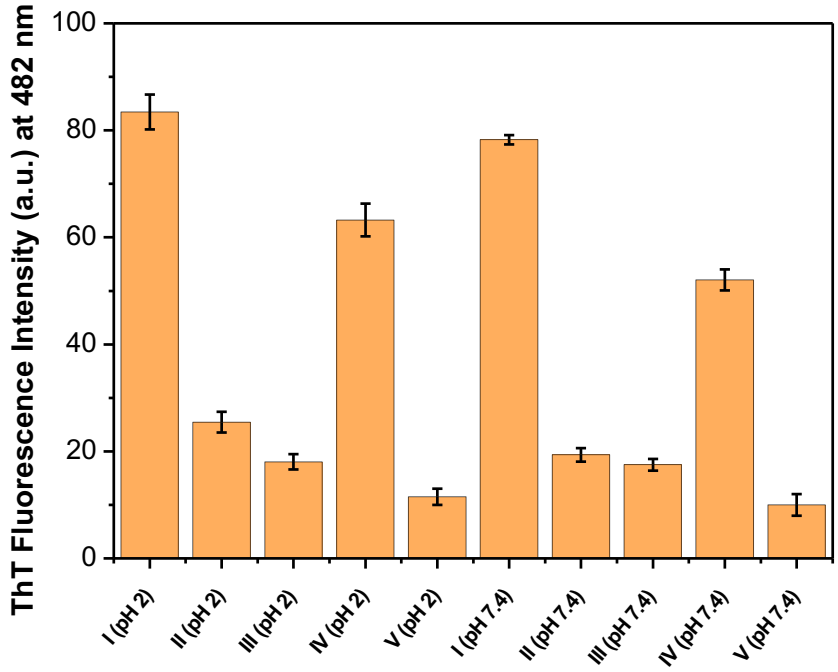

Fig. S11 ThT fluorescence assay of the individual peptide (I) and CDP-peptidomimetics (II-V) at pH 2.0 and 7.4 upon incubating the samples for 20 days and 37 °C temperature. ThT assay indicates self-aggregation potential of I and IV at both pH conditions, whereas, the peptidomimetics II, III, V possess negligible self-aggregation properties as compared to I and IV. The higher self-aggregation propensity of IV could be the reason for the enhanced fibrillation of I in the presence of IV

Characterizations of kd, Aβ14-23 (I) and peptidomimetics (II-V)

Table S1 HRMS and MALDI mass analysis.

Name	Sequence	Calculated exact mass	Observed mass	
			HRMS	MALDI
Fmoc-kd	Fmoc-cyclo(Asp-Lys)	465.1900	466.1790 $[M+H]^+$	-
I	His-Gln-Lys-Leu-Val-Phe-Phe-Ala-Glu-Asp	1231.6350	616.8319 $[M/2+H]^+$	1255.26 $[M+Na]^+$
II	His-Gln-Lys-Leu-Val-kd-Phe-Phe-Ala-Glu-Asp	1456.7463	729.3777 $[M/2+H]^+$	1458.26 $[M]^+$
III	His-Gln-Lys-Leu-Val-Phe-Phe-Ala-Glu-Asp-kd	1456.7463	729.8835 $[M/2+H]^+$ 486.9256 $[M/3+H]^+$	1458.59 $[M]^+$
IV	kd-His-Gln-Lys-Leu-Val-Phe-Phe-Ala-Glu-Asp	1456.7463	729.3808 $[M/2+H]^+$ 486.5907 $[M/3+H]^+$	1457.86 $[M]^+$
V	kd- His-Gln-Lys-Leu-Val-kd-Phe-Phe-Ala-Glu-Asp-kd	1906.9690	954.9907 $[M/2+H]^+$	1909.09 $[M+H]^+$

Table S2 Purification (HPLC) of Aβ14-23 (I) and peptidomimetics (II-V)

Samples	Gradient of the mobile phase	Flow rate (ml/min)	Retention time (min)	Purity (%)
I	5-95% MeCN (0.1% TFA) in H_2O (0.1% TFA) for 25 min	8	10.18	>99
II	5-95% MeCN (0.1% TFA) in H_2O (0.1% TFA) for 25 min	8	10.04	>99
III	5-95% MeCN (0.1% TFA) in H_2O (0.1% TFA) for 25 min	8	9.93	>99
IV	5-95% MeCN (0.1% TFA) in H_2O (0.1% TFA) for 25 min	8	10.04	>99
V	5-95% MeCN (0.1% TFA) in H_2O (0.1% TFA) for 25 min	8	10.27	>99

Table S3 List of the docking parameters: Binding energies and hydrogen bond distances between different atoms of the Aβ42 peptide and the ligand Akd^{NMC} (V).

Interacting Sites	**Bond distance (Å)**	**Category of Bond**	**Type of Bond**
Intermolecular Interactions **(Aβ42: V, Binding Energy: -5.2 Kcal/mole)**			
His14:H*^{S} - N-kd:O	2.02	Hydrogen Bond	Conventional Hydrogen Bond
His14:H*^{S} - Asp:O	2.43	Hydrogen Bond	Conventional Hydrogen Bond
Ala21:O - M-kd:H	2.69	Hydrogen Bond	Conventional Hydrogen Bond
Glu22:O*^{S} – N-kd:H	2.27	Hydrogen Bond	Conventional Hydrogen Bond
His14 - C-kd:H	3.56	Hydrophobic	π-σ
Val18 – N-kd	4.86	Hydrophobic	Alkyl
Leu17 - Ala:C	4.94	Hydrophobic	Alkyl
Ala21 – Phe2	4.36	Hydrophobic	π-Alkyl
Val18 – Phe1	5.19	Hydrophobic	π-Alkyl
Ala21 – Phe1	4.70	Hydrophobic	π-Alkyl

*^{S} = Side chain atoms of Aβ42 (left-side residues: Aβ42 and right-side residues: V)
Phe1 = ^{19}Phe of the ligand (V), Phe2 = ^{20}Phe of the ligand (V)

Table S4 List of the docking parameters and binding interactions for the docked structures of I:II, I:III, I:IV, and I:V.

Interacting Sites	Bond distance (Å)	Category of Bond	Type of Bond
Intermolecular Interactions (I:II, Binding Energy: -4.1 Kcal/mole)			
Glu22:O*^{S} - His:H	2.83	Hydrogen Bond	Conventional Hydrogen Bond
Glu22:O - His:H	1.99	Hydrogen Bond	Conventional Hydrogen Bond
Ala21:O - Gln:H	2.20	Hydrogen Bond	Conventional Hydrogen Bond
Val18:C*^{S} - Phe:O	3.07	Hydrogen Bond	Carbon Hydrogen Bond
Glu22:O*^{S} - His	3.63	Electrostatic	π-Anion
Phe20 - Val:C	3.62	Hydrophobic	π-σ
His14 – Phe2	5.02	Hydrophobic	π-π T-shaped
Val18 – Phe2	5.33	Hydrophobic	π-Alkyl
Intermolecular Interactions (I:III, Binding Energy: -4.1 Kcal/mole)			
Phe19:O – C-kd:H	1.79	Hydrogen Bond	Conventional Hydrogen Bond
Asp23:O*^{S} – C-kd:H	2.53	Hydrogen Bond	Conventional Hydrogen Bond
Phe19:O – C-kd:H	2.44	Hydrogen Bond	Conventional Hydrogen Bond
Gln15:O*^{S} -Glu :C	3.79	Hydrogen Bond	Carbon Hydrogen Bond
Phe19 – C-kd	5.21	Hydrophobic	π-Alkyl
Phe20 – C-kd	4.25	Hydrophobic	π-Alkyl
Intermolecular Interactions (I:IV, Binding Energy: -3.1 Kcal/mole)			
Gln15:HN – N-kd:O	2.85	Hydrogen Bond	Conventional Hydrogen Bond
Gln15:O*^{S} -Lys:H	1.99	Hydrogen Bond	Conventional Hydrogen Bond
Gln15:O*^{S} -Lue:H	2.63	Hydrogen Bond	Conventional Hydrogen Bond
Leu17:C*^{S} – Phe2	3.74	Hydrophobic	π-σ
LYS16 – Phe1	4.92	Hydrophobic	π-Alkyl
Intramolecular Interactions within IV			
Leu:N - Asp:O	3.20	Hydrogen Bond	Conventional Hydrogen Bond
Asp:N - Asp:O	3.17	Hydrogen Bond	Conventional Hydrogen Bond
Asp:OH- Glu:O	3.09	Hydrogen Bond	Conventional Hydrogen Bond
Asp:O - Lys:N	2.99	Hydrogen Bond	Conventional Hydrogen Bond
Glu:O - His:N	2.88	Hydrogen Bond	Conventional Hydrogen Bond
Lys:N - Lys:O	2.97	Hydrogen Bond	Conventional Hydrogen Bond
kd:O - Lys:N	3.08	Hydrogen Bond	Conventional Hydrogen Bond
kd:N - kd:O	3.11	Hydrogen Bond	Conventional Hydrogen Bond
His:N - Gln	3.91	Hydrogen Bond	π-Donor Hydrogen Bond
Leu:C – Phe1	3.65	Hydrophobic	π-σ
Intermolecular Interactions (I:V, Binding Energy: -4.9 Kcal/mole)			
His14:H*^{S} - Asp:O	1.83	Hydrogen Bond	Conventional Hydrogen Bond
Phe19:O - His:H	2.80	Hydrogen Bond	Conventional Hydrogen Bond
Asp23:O - Leu:H	2.81	Hydrogen Bond	Conventional Hydrogen Bond
Asp23:O*^{S} - Val:H	2.78	Hydrogen Bond	Conventional Hydrogen Bond
Glu22:O – M-kd:H	2.13	Hydrogen Bond	Conventional Hydrogen Bond
Ala21:OH – M-kd:H	2.35	Hydrogen Bond	Conventional Hydrogen Bond
Asp23:O*^{S} – N-kd:H	2.90	Hydrogen Bond	Conventional Hydrogen Bond
Asp23:C – M-kd:O	2.66	Hydrogen Bond	Carbon Hydrogen Bond
Glu22:O*^{S} - Val:C	3.17	Hydrogen Bond	Carbon Hydrogen Bond
Ala21:O - Glu:C	3.08	Hydrogen Bond	Carbon Hydrogen Bond
Leu17 – Phe2	5.12	Hydrophobic	π-Alkyl

*^{S} = Side chain atoms of I (left-side residues: I and right-side residues: II/III/IV/V)
Phe1 = ^{19}Phe of the ligand (II-V), Phe2 = ^{20}Phe of the ligand (II-V)

HPLC chromatogram, HRMS and MALDI mass of Aβ14-23 (I)

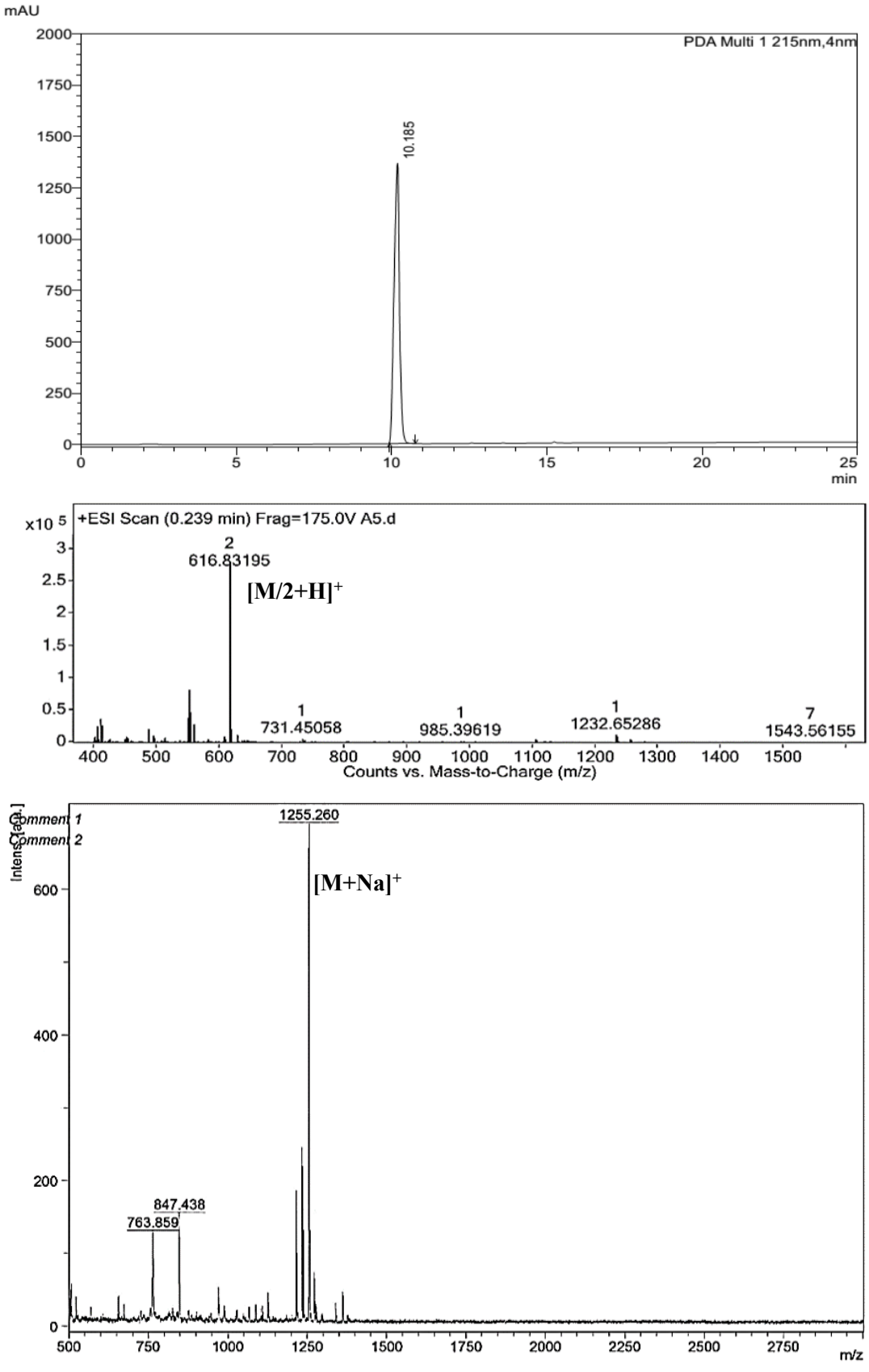

HPLC chromatogram, HRMS, and MALDI mass of Akd^{M} (II)

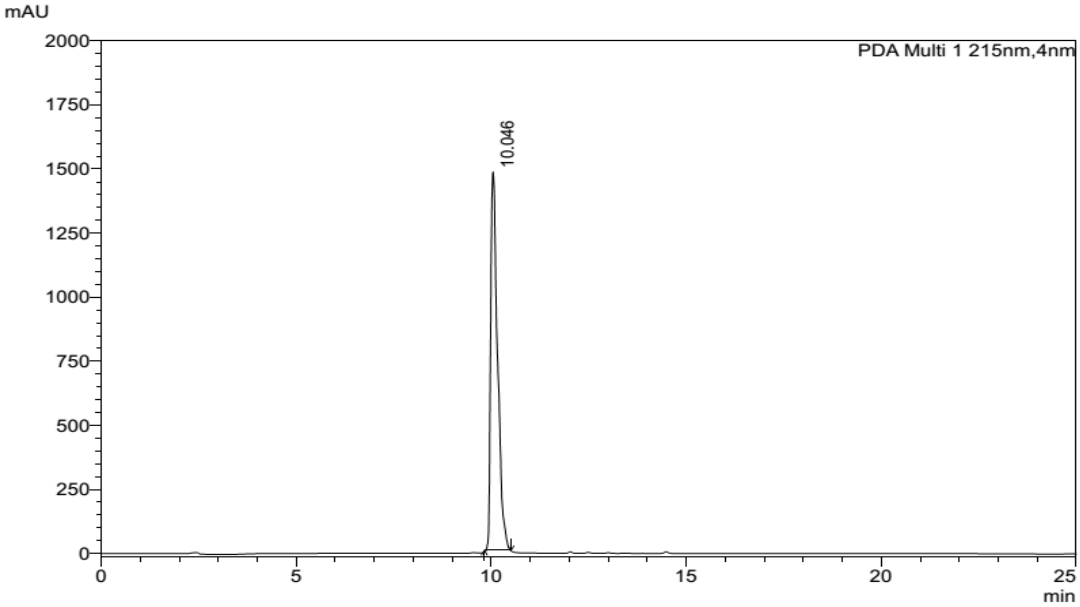

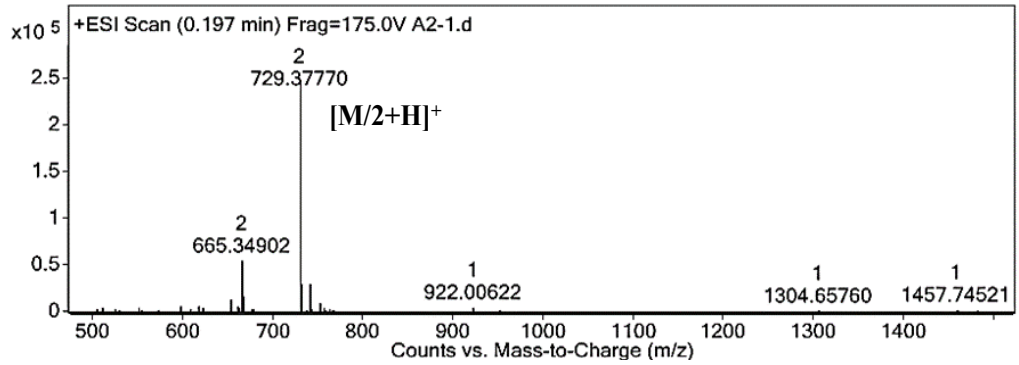

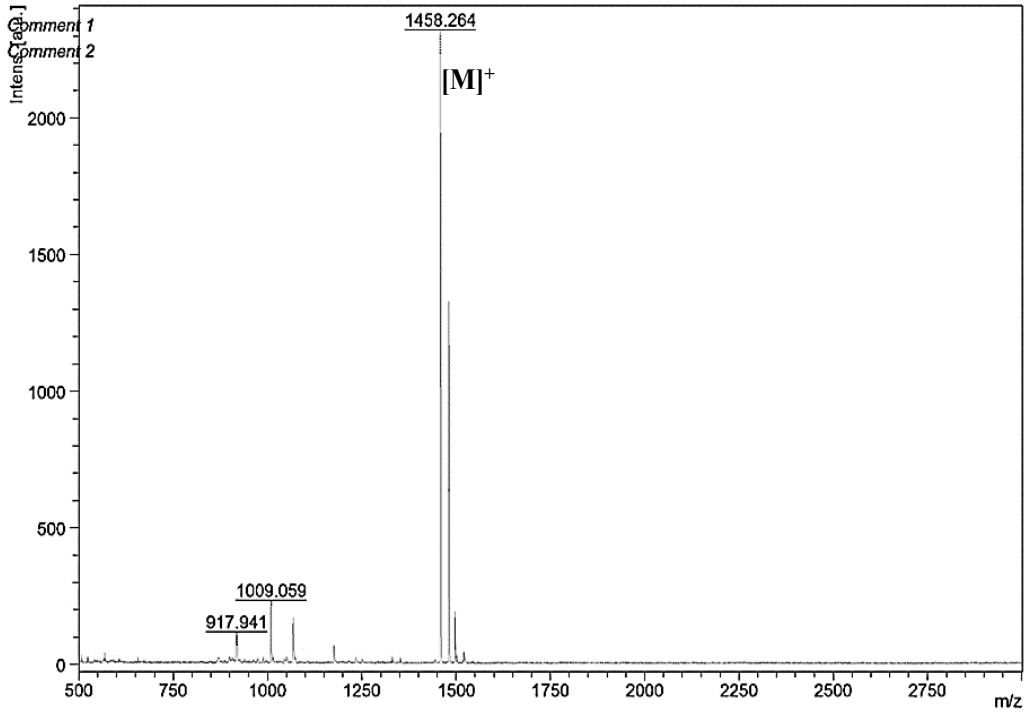

HPLC chromatogram, HRMS and MALDI mass of Akd^{C} (III)

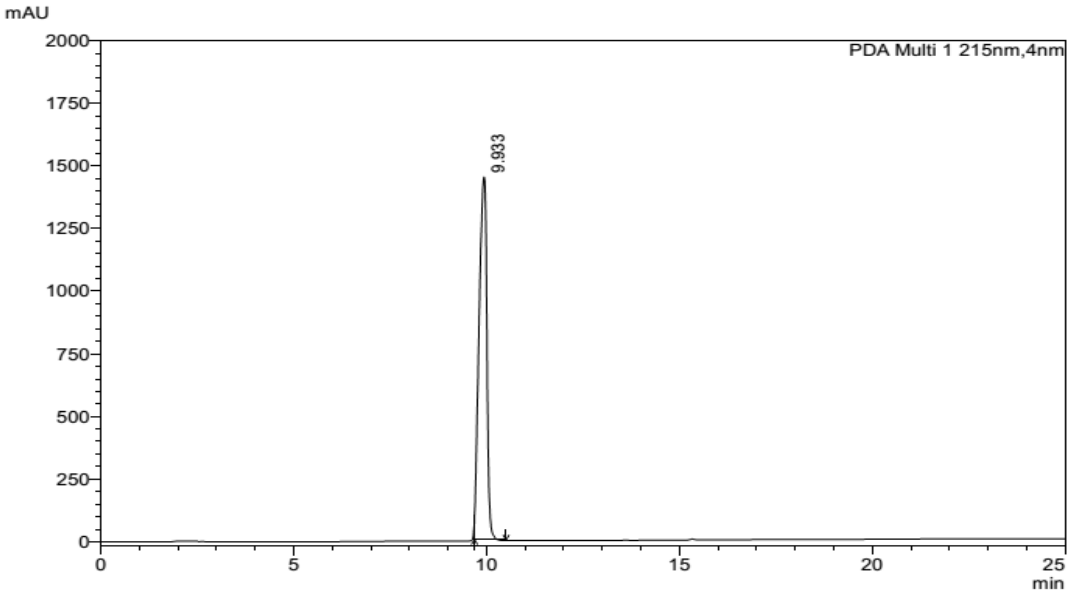

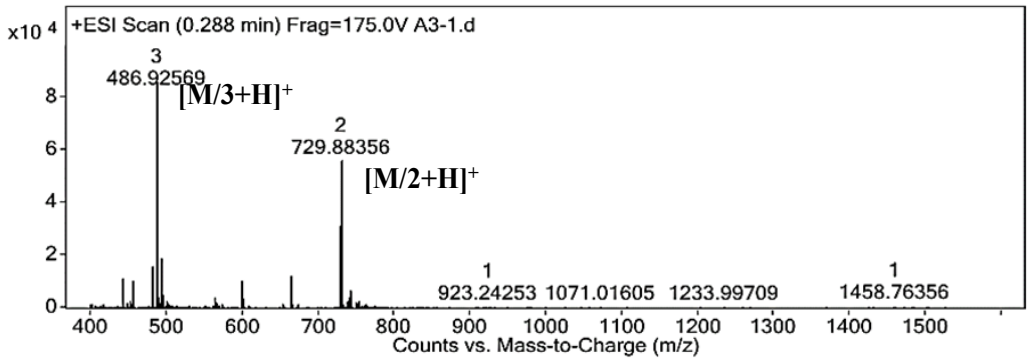

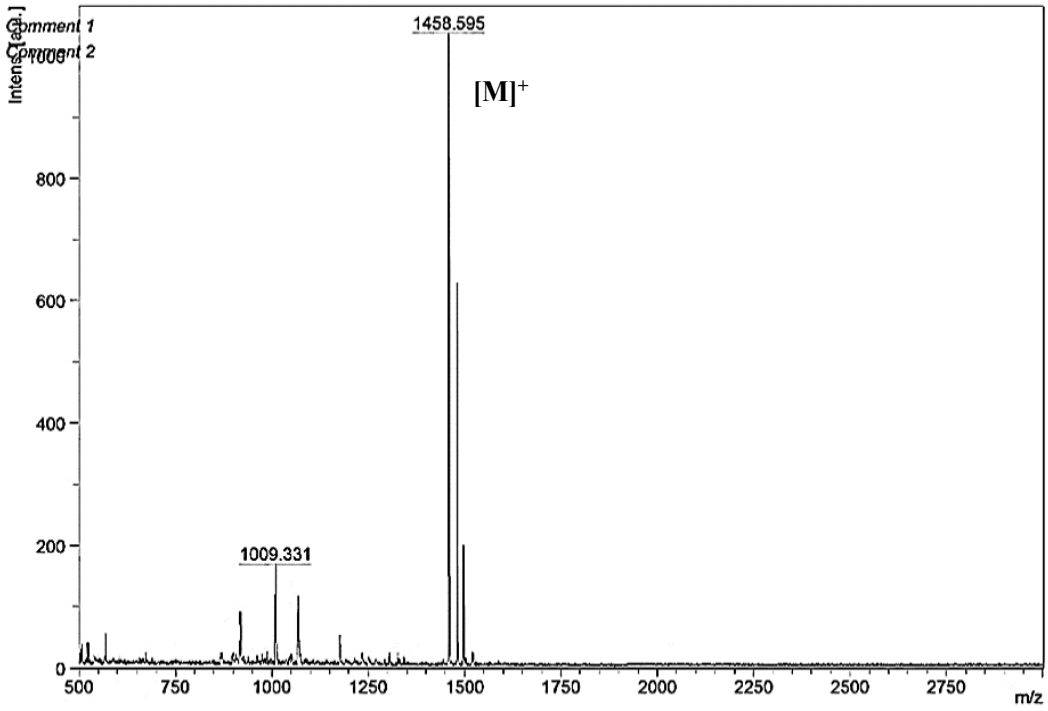

HPLC chromatogram, HRMS and MALDI mass of Akd^N (IV)

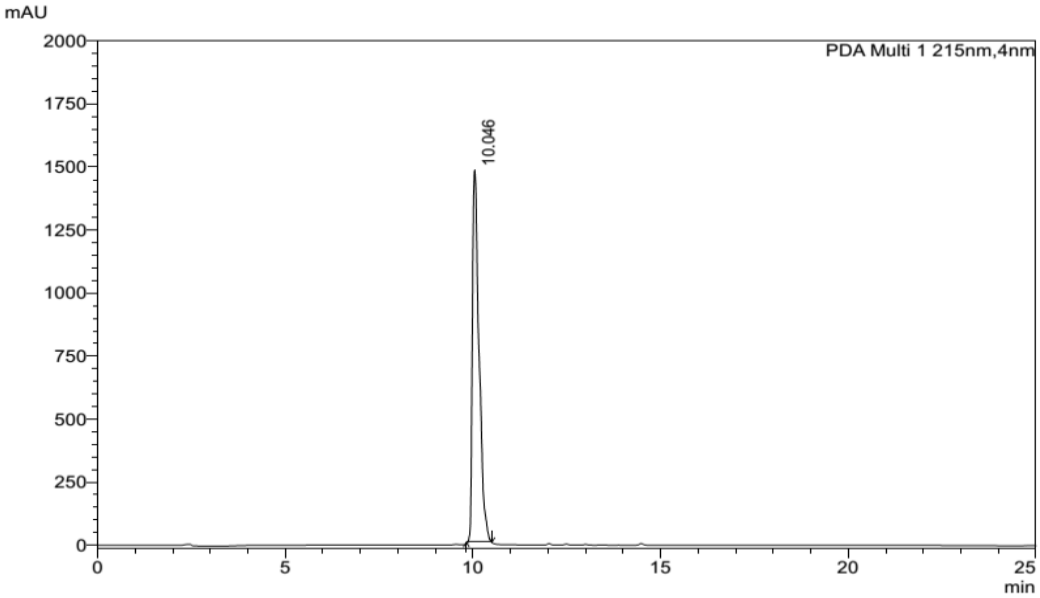

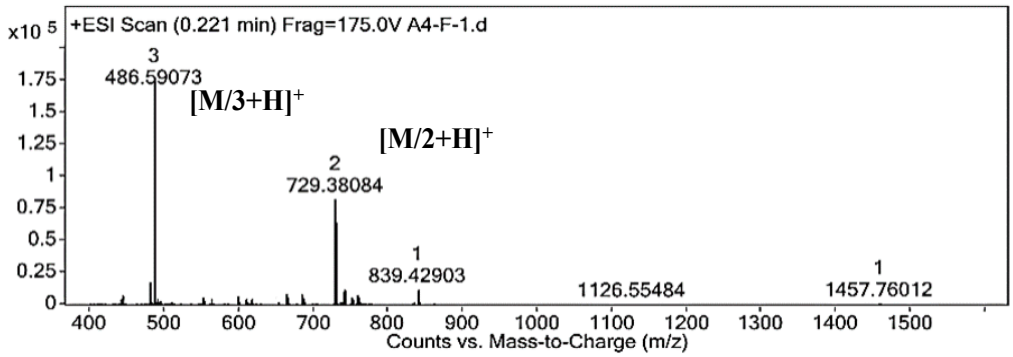

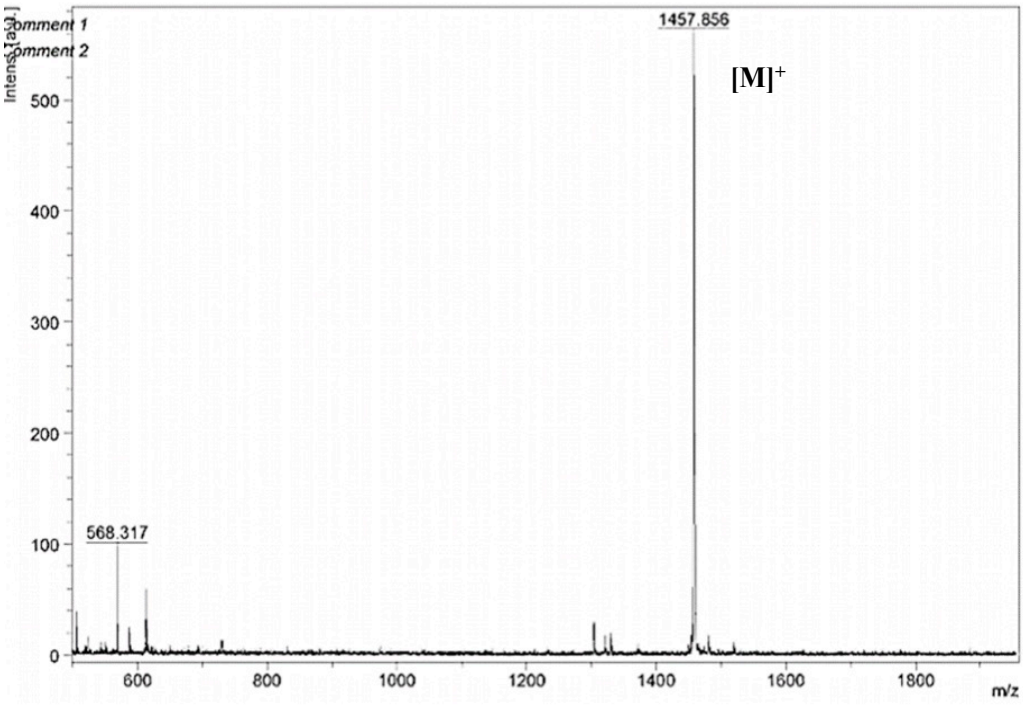

HPLC chromatogram, HRMS and MALDI mass of Akd^{NMC} (V)

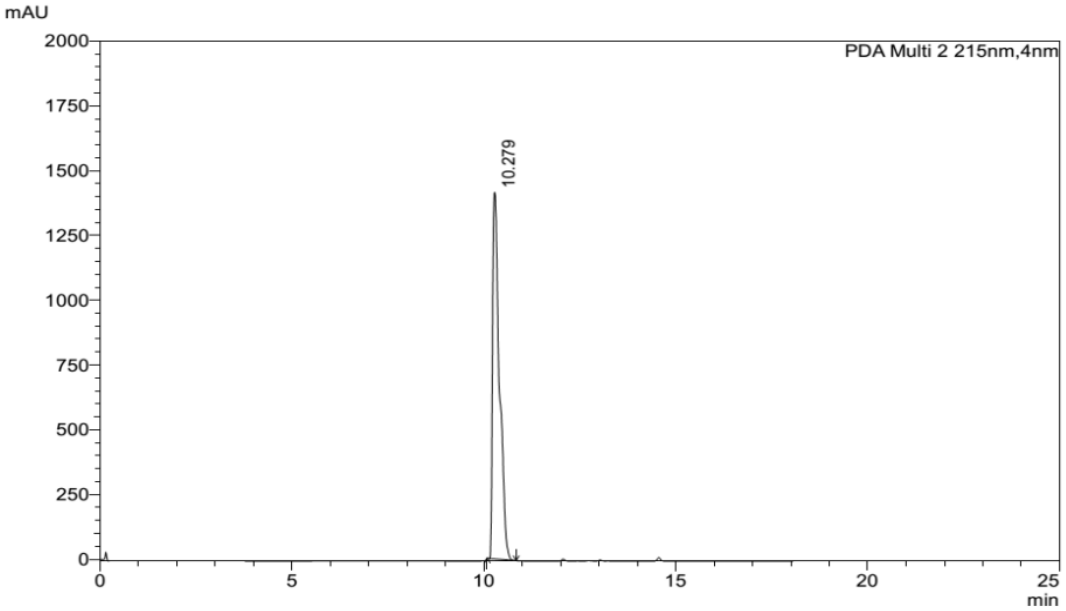

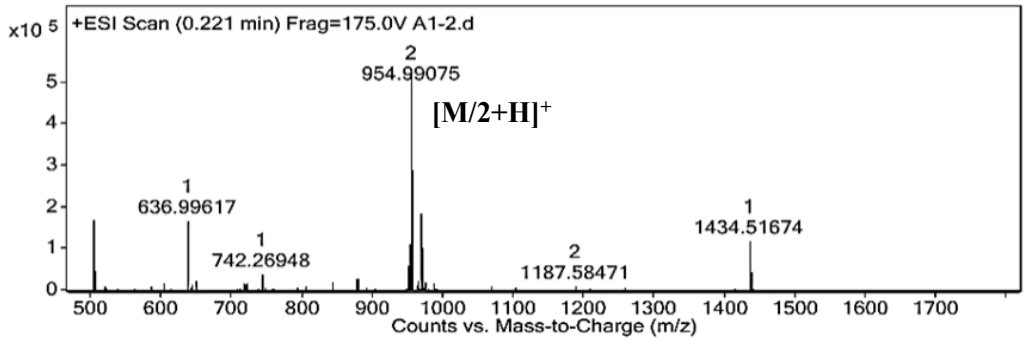

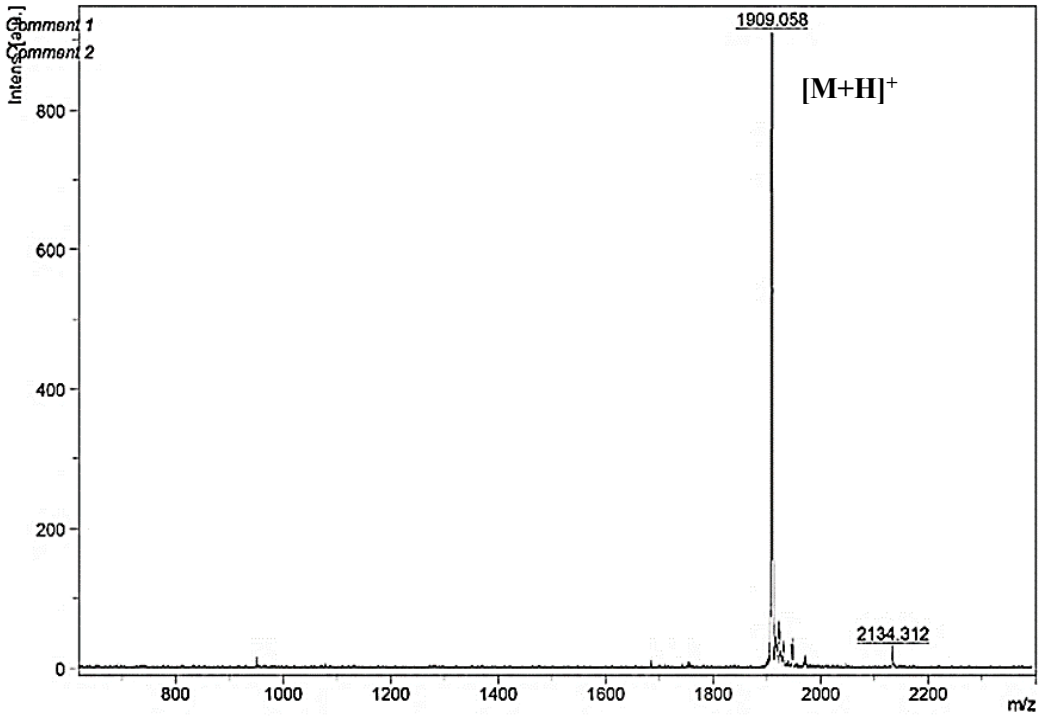

^{1}H and ^{13}C NMR and HRMS data of Fmoc-kd

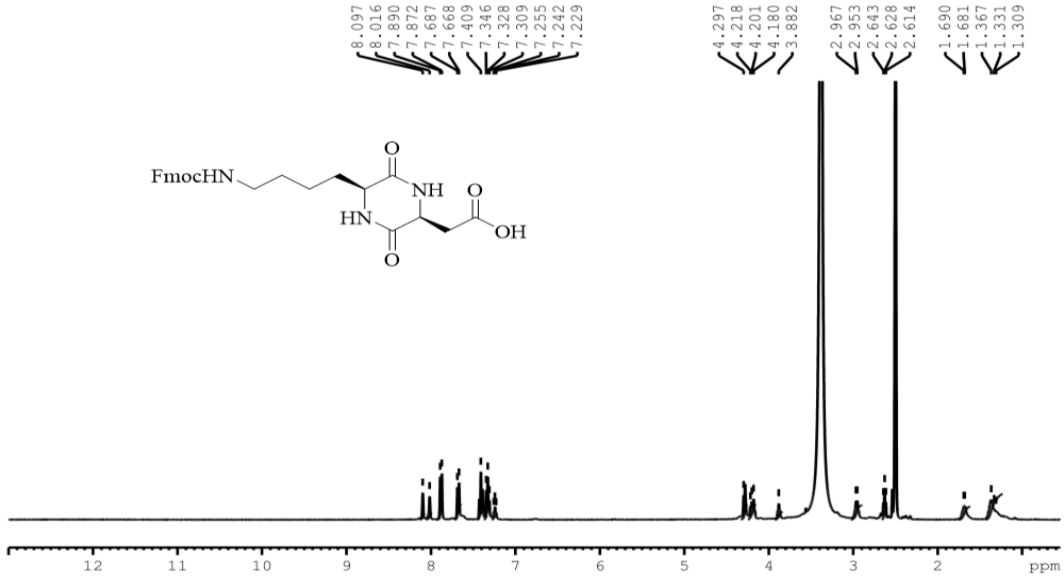

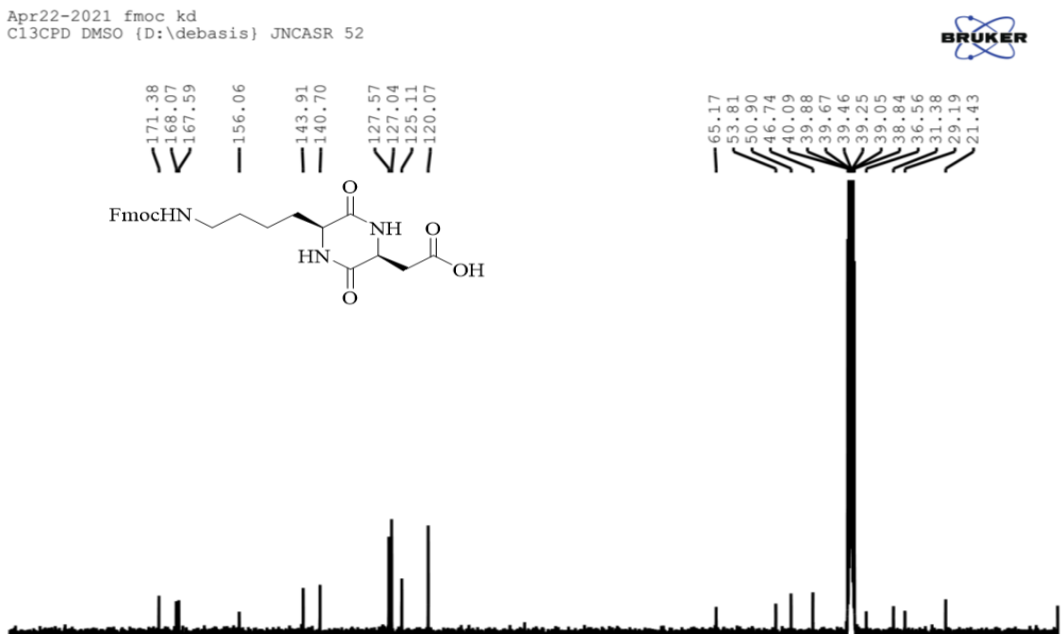

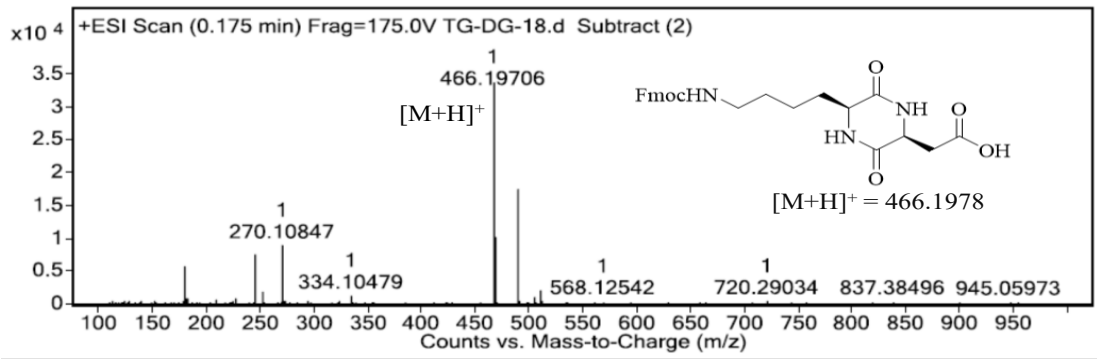

References

1. O. Trott and A. J. Olson, AutoDock Vina: improving the speed and accuracy of docking with a new scoring function, efficient optimization and multithreading. *J. Comput. Chem.*, 2010, **31**, 455-461.

2. G. M. Morris, R. Huey, W. Lindstrom, M. F. Sanner, R. K. Belew, D. S. Goodsell and D. S. Olson, AutoDock4 and AutoDockTools4: Automated docking with selective receptor flexibility. *J. Comput. Chem.*, 2009, **30**, 2785-2791.